Al-Khwarizmi Engineering Journal, Vol. 4, No. 4, PP 106-121 (2008)

Al-Khwarizmi Engineering Journal

Study The Influence of Forming Conditions Like Deformation Speed on Void Closure in Open Die Forging

Alaa Hassan Ali

Department of Materials Engineering/ University of Technology

(Received 10 June 2007; accepted 10 September 2008)

Abstract

This paper presents an investigation to the effect of the forming speed on healing voids that inhabit at various size in an ingot. The study was performed by using finite element method with bilinear isotropic material option, circular type voids were considered. The closure index was able to predict the minimum press force necessary to consolidate voids and the reduction. The simulation was carried out, on circular cross-section lead specials containing a central void of different size. At a time with a flat die, different ratio of inside to outside radius was taken with different speed to find the best result of void closure.

Keywords:

1. Introduction:

Casting is the method used to shape bulk of engineering materials due to simplicity and possibility of casting large products. The defects in casting are shrinkage, gas porosity, hot tears, alloy segregation and inclusions [1]. The defects by solidification shrinkage and gas porosity are relatively different to control. The void formed in the product must be eliminated by the application of compression loads compatible with plastic deformation.

Forging is classified as closed die and open die forging. In closed die forging, a compressive force is applied on the work piece and forced to take the shape of the die surface or impression.

Open die forging is a process used to produce huge turbine shafts, nuclear reactors, vessels and pressure value [2]. These parts should have good toughness and fatigue strength.

Most failures of engineering components can be initiated by concentration of stresses of internal microscopic voids or inclusions, therefore the strategy is to close and consolidate these internal defects completely [3].

Closure of voids and consolidation of internal defects is a very significant issue for some reasons like void constitutes the weakest portion of the component, and act as stress raisers, which promote fatigue.

The finite element method (FEM) is a comprehensive tool which is flexible and capable of tracing material flow and able to investigate contours of stresses and strain, even in cases of linear and non-linear material properties [4].

2. Theoretical consideration and analysis:

The efficient method of analysis for metal forming should be capable of predicting the effect of various parameters on metal flow characteristics [5].

In this regard, the rigid viscoplastic defect formation in metal forming.

In simulating, the void closure in forging the assumptions taken for the material and the process such as an isotropic and homogenous, rigid perfectly plastic, the friction between the work piece and the die is considered to obey coulomb friction low (sliding only), plane strain and isothermal process.

For (2D) finite element surface to surface analysis, Ansys software utilizes two distinct contact surfaces, the rigid surface referred to as" target" surfaces which is modeled with element type

"targe 169" or the deformable body surface is referred as" contact" element type contact for 2D . Large strain solid the element type visco 106 is used (four-node nonlinear solid).
For quadrilateral element, the displacements are interpolated as follows [6]:

$$u = \sum_{\tau=1}^{4} niui \qquad \ldots(1)$$

$$v = \sum_{i=1}^{4} nivi \qquad \ldots(2)$$

Strains are obtained from the displacements:-

$$\varepsilon_x = \frac{\partial_u}{\partial_x} = \sum_{i=1}^{4} \frac{\partial_{ni}}{\partial_x} ui \qquad \ldots(3)$$

$$\varepsilon_y = \frac{\partial_v}{\partial_x} = \sum_{i=1}^{4} \frac{\partial_{ni}}{\partial_y} vi \qquad \ldots(4)$$

$$\varepsilon_{xy} = \frac{\partial_u}{\partial_y} + \frac{\partial v}{\partial_x} = \sum_{i=1}^{4} \left(\frac{\partial_{ni}}{\partial_y} ui + \frac{\partial_{ni}}{\partial_x} vi \right) \qquad \ldots(5)$$

$$\underline{\varepsilon} = \begin{bmatrix} \frac{\partial_{n1}}{\partial_x} 0 \frac{\partial_{n2}}{\partial_x} 0 \frac{\partial_{n3}}{\partial_x} 0 \frac{\partial_{n4}}{\partial_x} 0 \\ 0 \frac{\partial_{n1}}{\partial_y} 0 \frac{\partial_{n2}}{\partial_y} 0 \frac{\partial_{n3}}{\partial_y} 0 \frac{\partial_{n4}}{\partial_y} \\ \frac{\partial_{n1}}{\partial_y} \frac{\partial_{n1}}{\partial_x} \frac{\partial_{n2}}{\partial_y} \frac{\partial_{n2}}{\partial_x} \frac{\partial_{n3}}{\partial_y} \frac{\partial_{n3}}{\partial_x} \frac{\partial_{n4}}{\partial_y} \frac{\partial_{n4}}{\partial_x} \end{bmatrix} \underline{\delta} \qquad \ldots(6)$$

where Ni=shape function for the node i
N1= (1- ζ) (1- η),
N2=ζ(1- η),
N3= ζ η and N4=η (1- ζ)

$$\underline{\varepsilon} = \left[\varepsilon_x \varepsilon_y \varepsilon_{xy} \right] \qquad \ldots(7)$$

$$\underline{\delta} = \left[u1v1u2v2u3v3u4v4 \right] \qquad \ldots(8)$$

Equation (6) can be expressed as:

$$\underline{\varepsilon} = \underline{B}.\underline{\delta} \qquad \ldots(9)$$

$$\sigma = \underline{D}\varepsilon = DB\delta \qquad \ldots(10)$$

$$D = \frac{E}{(1+\nu)(1-\nu)} \begin{bmatrix} 1-\nu\nu 0 \\ \nu 1-\nu 0 \\ 00\frac{1-2\nu}{2} \end{bmatrix} \qquad \ldots(11)$$

Strain energy U = $\frac{1}{2}\iiint \underline{\varepsilon}^t \underline{\sigma}\, dxdydz$ …(12)

Hence U = $\frac{1}{2}\iiint (\underline{B\delta})^t DB\delta dxdydz$

By substitution of equation (2) and (10) into (12)

$$U = \frac{1}{2\iiint \underline{\delta}^t} BDB\delta dxdydz \qquad \ldots(13)$$

Also, the work done by external forces ,

$$W = \underline{\delta}^t F \qquad \ldots(14)$$

The total potential energy for the element

$$\chi = U - W \qquad \ldots(15)$$

$$\chi = \underline{\delta}^t \frac{1}{2}\iiint \underline{B}^t DB\delta dxdydz - \underline{\delta}^t F \qquad \ldots(16)$$

Applying the minimum energy theorem, $\frac{\partial_x}{\partial \underline{\delta}} = 0$

Equation (16) becomes:

$$\iiint \underline{B}^t \underline{D}\, \underline{B}\, \underline{\delta}\, dxdydz - F = 0 \qquad \ldots(17)$$

$$\underline{Ke}\,\delta = F \qquad \ldots(18)$$

Where $\underline{K}\, e = \iiint \underline{B}^t \underline{D}\, \underline{B}\, dxdydz$

For plane strain; dz = constant =t (element thickness)

Thus $\underline{K}\, e = \iint tB^t DBdxdy$ …(19)

In large stain solids the Cauchy stress σ in equation 10 is decomposed into deviatory part plus pressure part:

$$\underline{\sigma} = \underline{\sigma}^{-} - [q]p \qquad \ldots(20)$$

$\underline{\sigma}^{-}$ = Cauchy stress deviator

$[q]$ = [1 11 0 0 0]

$$P = \left(\frac{\sigma_x + \sigma_y + \sigma_z}{3} \right).$$

The pressure is independently interpolated.

3. Simulation and Results:

The closure and pressing force plot, versus displacement are used to investigate the effect of different speed on closure of voids located at specified positions singly at a time and collectively. In forging process, the important step is the step where the void is healed completely such that avert the possibility of reopening of void during manipulation process. Accordingly, the simulation where made up to the instant of closure of voids. The model built as a half of circle containing a central void as shown in fig. (1), the simulation procedures taken according to the following conditions:

1. Taken the void as central void of the cylindrical ingot with 0.2 ratio of the inner to outer radius and different speeds of closure as follows:-
   - A- Speed of 0.2 mm/min the results are shown in figs. (2, 3, 4, 5, 6, 7)
   - B- Speed of 2 mm/min the results are shown in figs. (8, 9, 10, 11, 12, 13, 14, 15, 16)
   - C- Speed of 20 mm/min the results are shown in figs. (17, 18, 19, 20, 21, 22, 23, 24, 25)
2. Taken the void as a central void of the cylindrical ingot with 0.3 ratio and the different speeds of closure representative as follows:
   - A- Speed of 0.2 mm/min the results are shown in figs. (26, 27, 28, 29, 30, 31, 32, 33, 34)
   - B- Speed of 2mm /min the results are shown in figs. (35, 36, 37, 38, 39, 40, 41)
   - C- Speed of 20 mm/min the results are shown in figs. (42, 43, 44, 45, 46, 47, 48, 49, 50)
3. Taken the void as a central void of the cylindrical ingot with of 0.4 ratio with the different speeds of closure as follows:
   - A- Speed of 0.2 mm/min the results are shown in figs. (51, 52, 53, 54, 55, 56, 57, 60, 61)
   - B- Speed of 2 mm/min the results are shown in figs. (62, 63, 64, 65, 66, 67, 68, 69)
   - C- Speed of 20 mm/min the results are shown in figs. (70, 71, 72, 73, 74, 75, 76, 77, 78)
4. Figures (A to D) represent the relation between the speed and displacement in (y) direction, stress (σ_y), strain and hydrostatic pressure for all ratio.

4. Discussions and Conclusions:

The results can get from the above figures summarized as follows:

1- From the force – displacement curves, it can be observed that:
   - A- For void closure decrease with increase the ratio with the same closure speeds, this shown in figs. (2, 8, 17).
   - B- With the same ratio the closure speed increase with increase of closure displacement, this shown in figs. (26, 35, 42), and also the same results of others ratio shown in figs. (51, 62, 70).

2- The von misses equivalent stress (σ_e) for each ratio with different speeds can be shown in figs. (4, 11, 20, 29, 37, 45, 54, 65, 73), highest stress concentrated near central void for highest closure speed (20 mm/min) for all ratios and also highest void closure.

3- For the deformation in (y) direction (uy) for all ratios are shown in figs. (3, 10, 19, 28, 36, 48, 57, 66, 75), it can be observed that highest deformation concentrated at the bottom of the ingot with highest speed at all ratios stages which cause best void closure with highest speed and ratio.

4- When compare the result shown in figs.(16, 25, 34, 42, 54, 63, 72, 81) for strain in (y) direction it can observed with same conditions that the highest (ε_y) happened on the highest speed at highest third ratio which also cause highest void closure .

5- The same result also confined to the hydrostatic pressure shown in figs. (7, 14, 23, 32, 40, 52, 61, 70, 79), it is observed that the highest pressure concentrated also in the bottom of the ingot and at the edge of the central void with highest void closure also.

6- From the points mentioned above it can be conclusion that the voids healed by the best result when used high speed with highest ratio of central void radius to outer radius of cylindrical ingot.

7- Figures A to D shows the relation of the speed with displacement in y direction in fig. (A) which shows that the increasing of displacement occurs with increasing the speed at highest ratio. Fig. B shows that the more the speed the more the stress at maximum ratio. The same behavior occurs in fig. C & D that with increasing of speed cause increasing each of strain and hydrostatic pressure at highest ratio also.

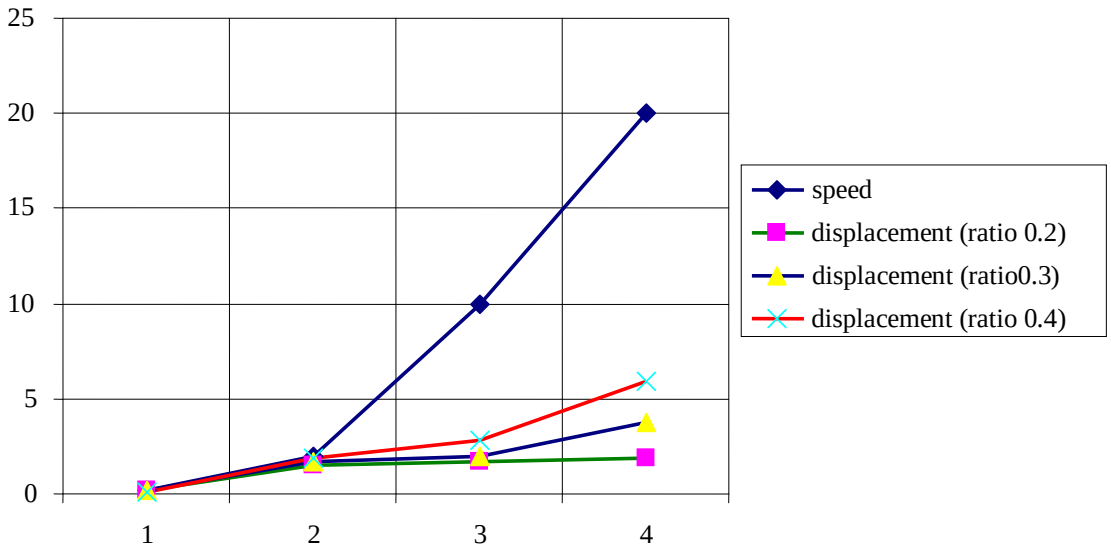

Fig.A. Speed & Displacement (Y).

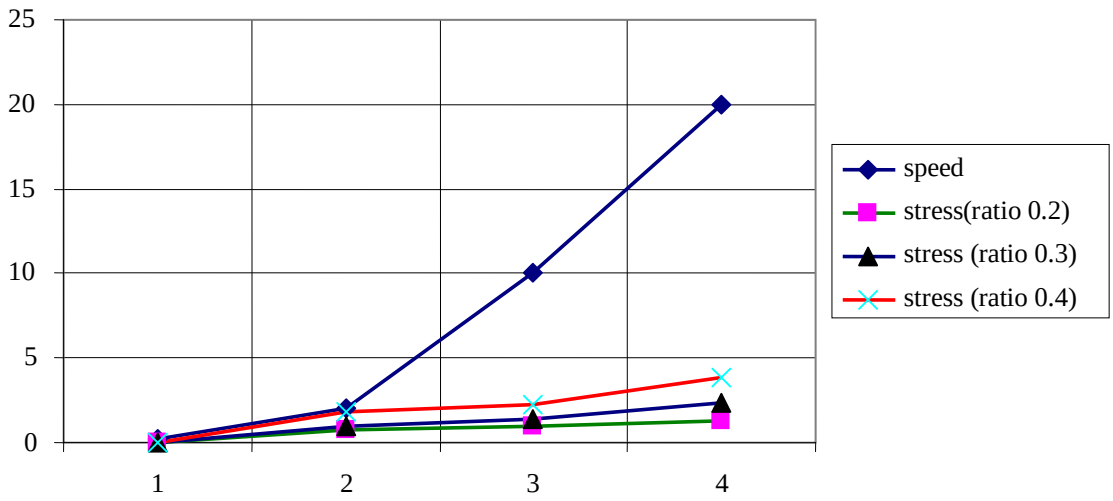

Fig. B. Speed & Stress (Y)

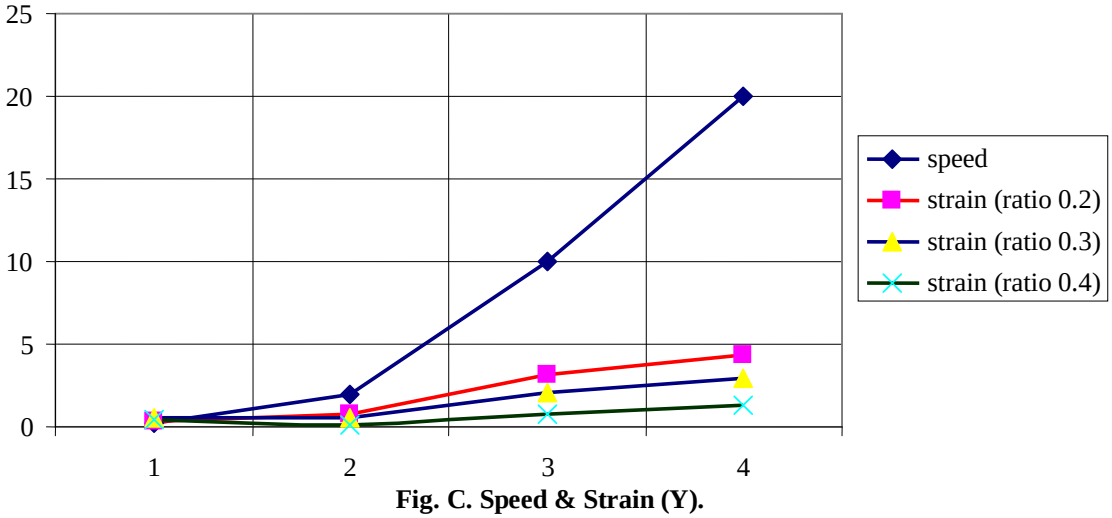

Fig. C. Speed & Strain (Y).

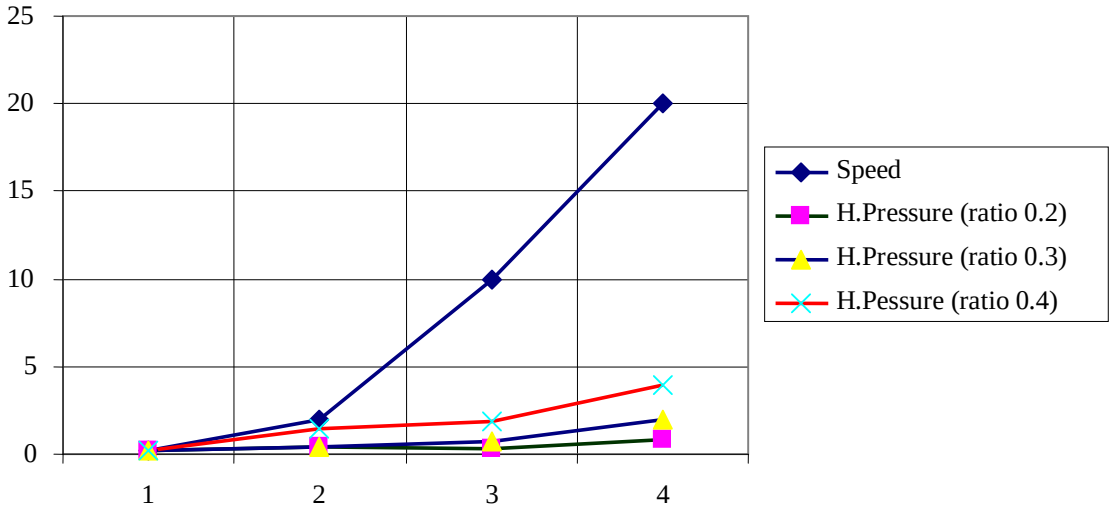

Fig. D. Speed & Hydrostatic Pressure.

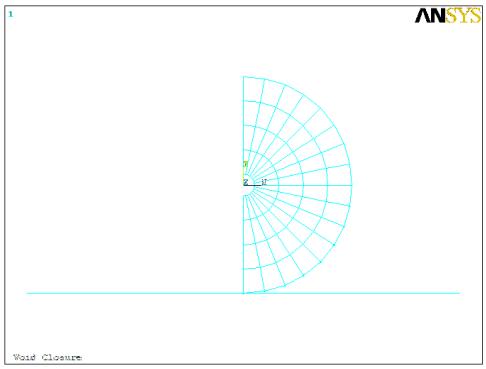

Fig. 1

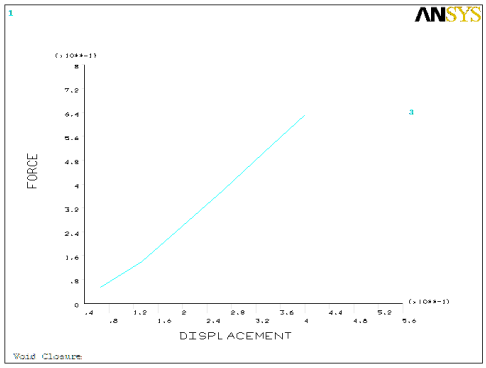

Fig. 2

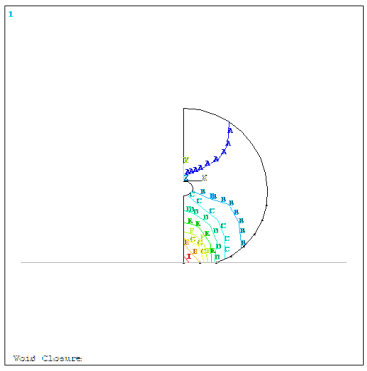

Fig. 3

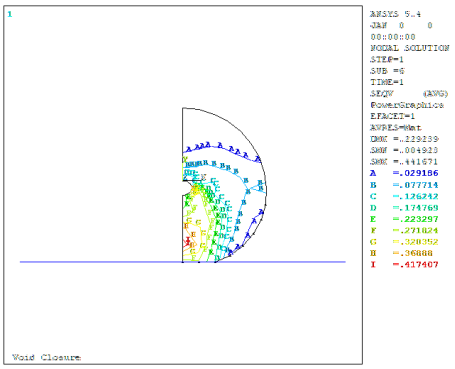

Fig. 4

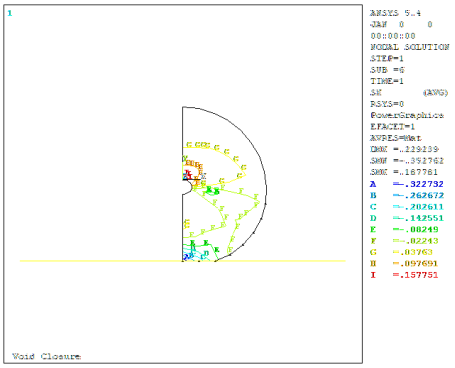

Fig. 5

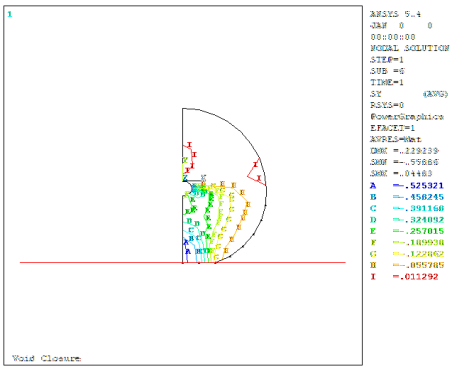

Fig. 6

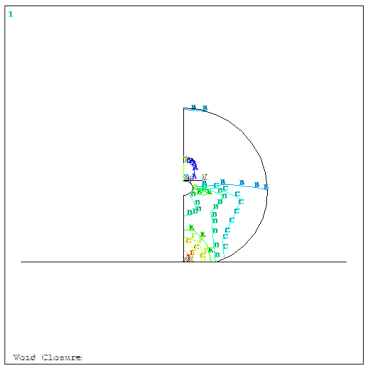

Fig. 7

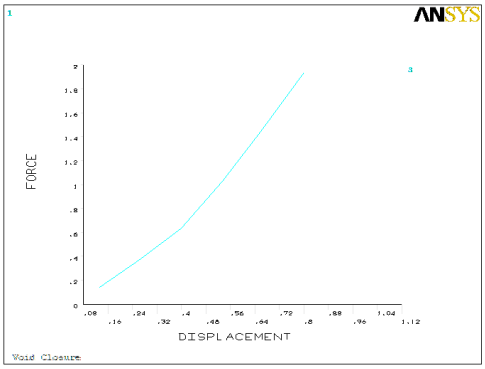

Fig. 8

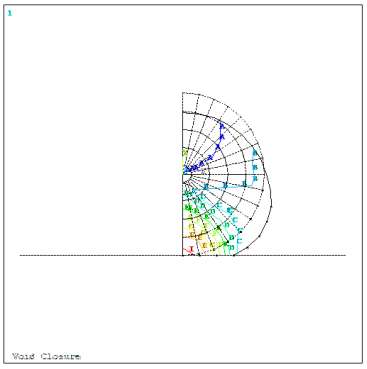

Fig. 9

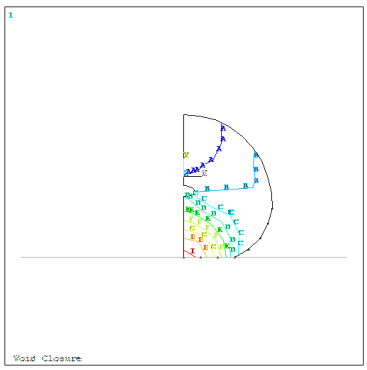

Fig. 10

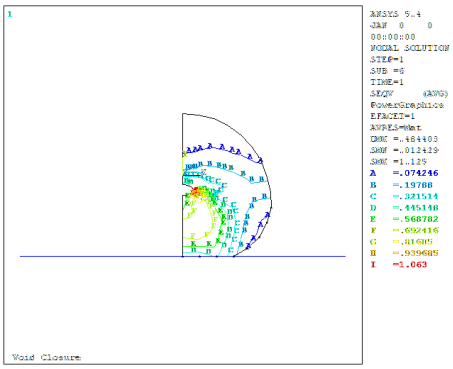

Fig. 11

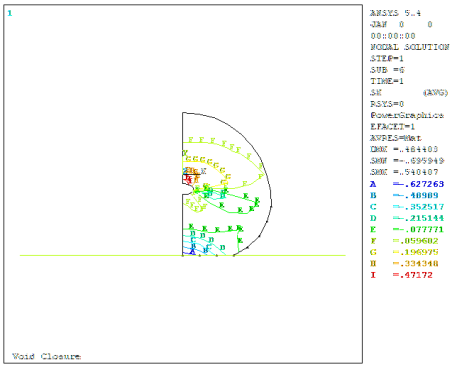

Fig. 12

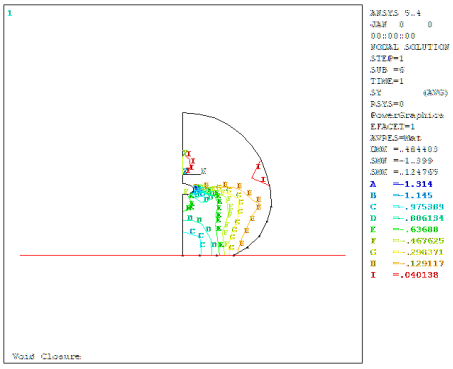

Fig. 13

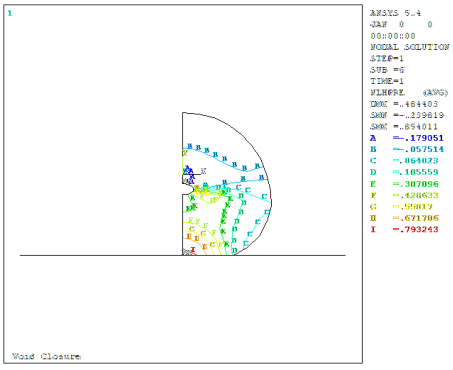

Fig. (14)

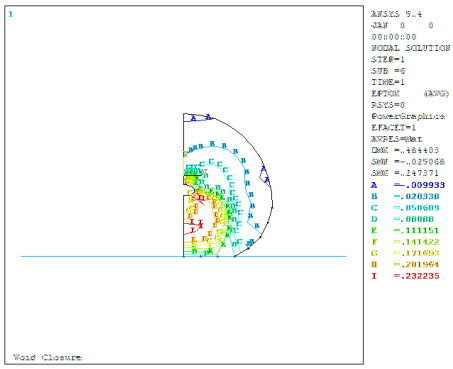

Fig. 15

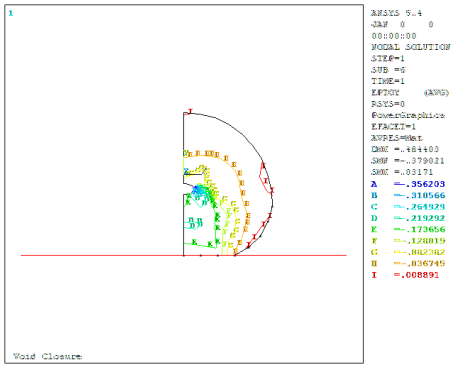

Fig. 16

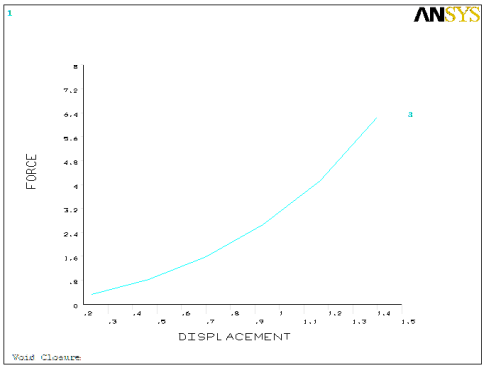

Fig. 17

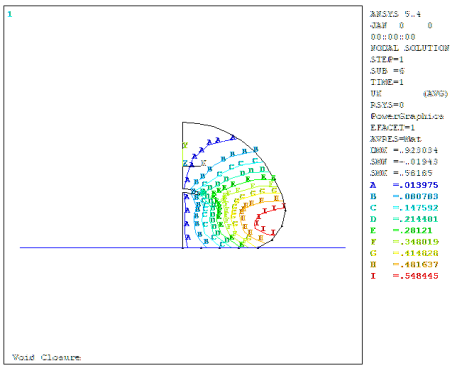

Fig. 18

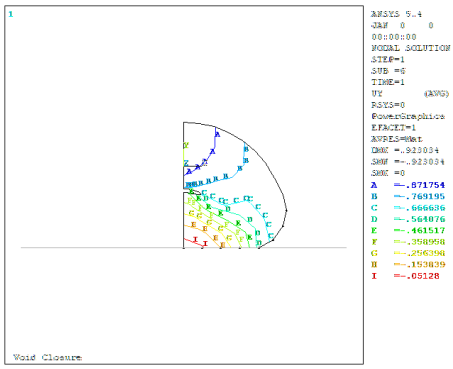

Fig. 19

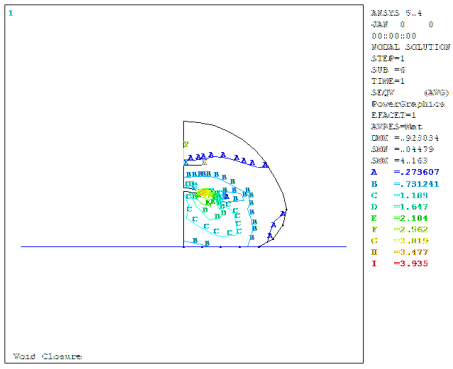

Fig. 20

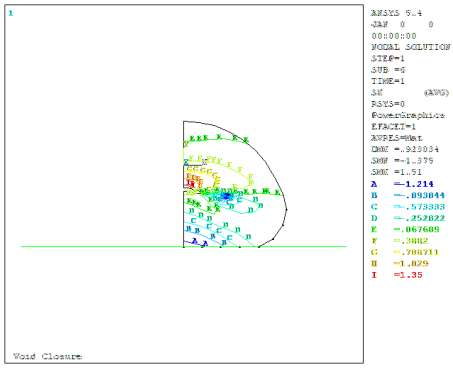

Fig. 21

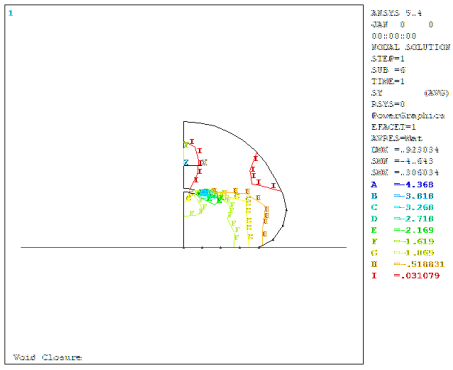

Fig. 22

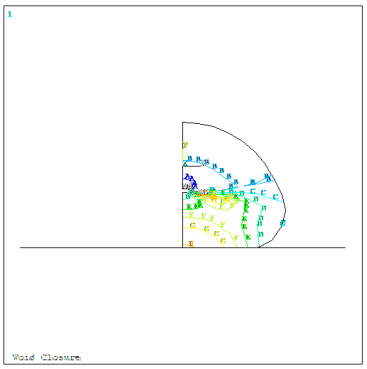

Fig. 23

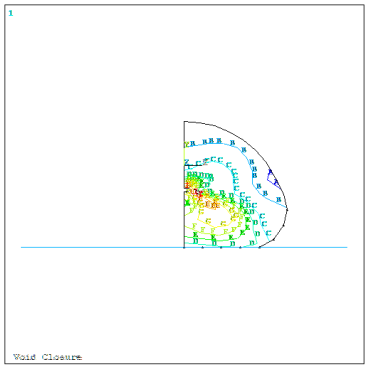

Fig. 24

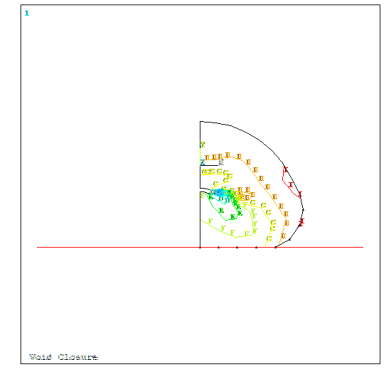

Fig. 25

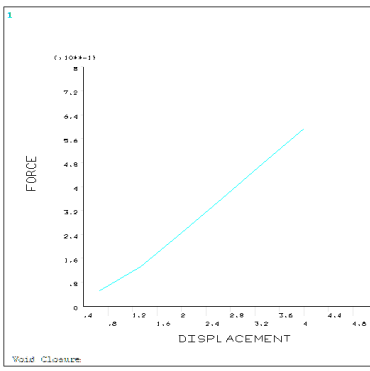

Fig. 26

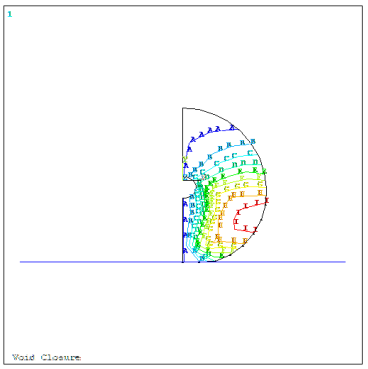

Fig. 27

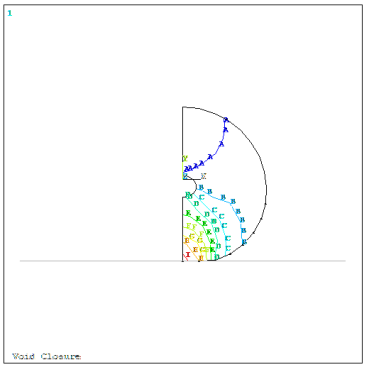

Fig. 28

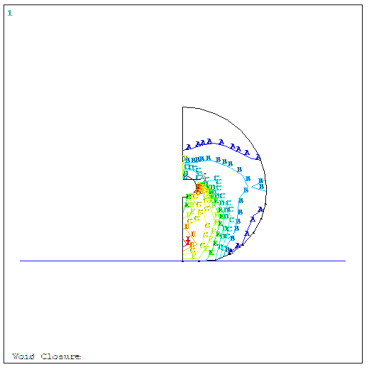

Fig. 29

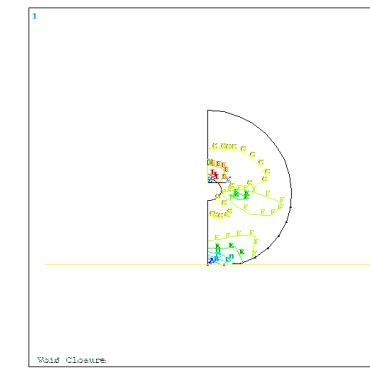

Fig. 30

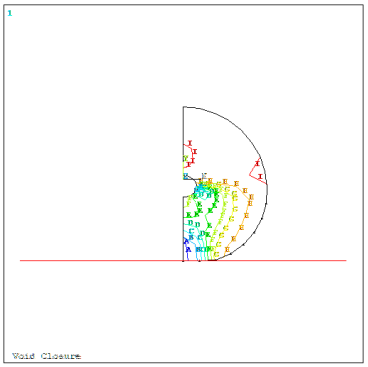

Fig. 31

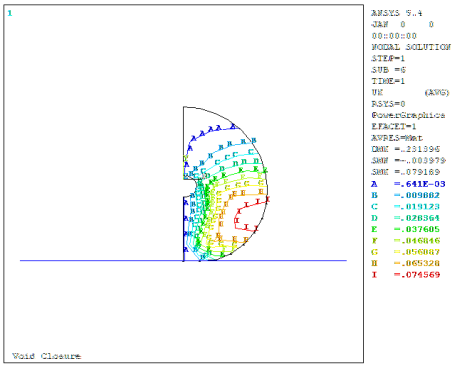

Fig. 35

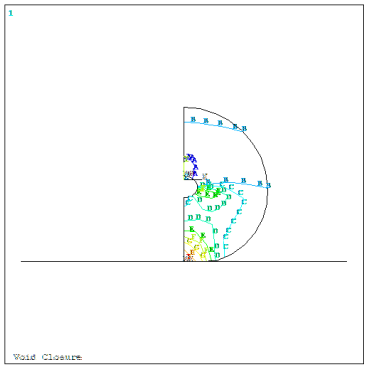

Fig. 32

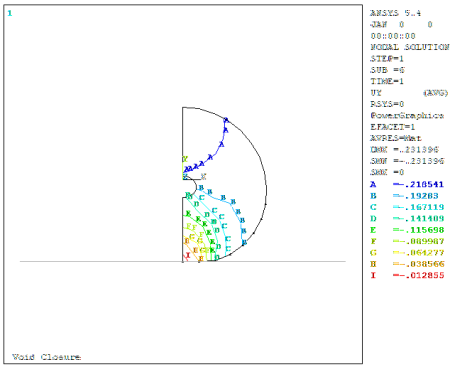

Fig. 36

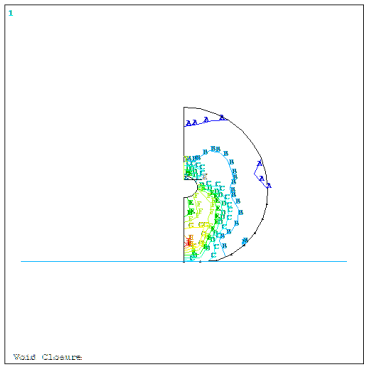

Fig. 33

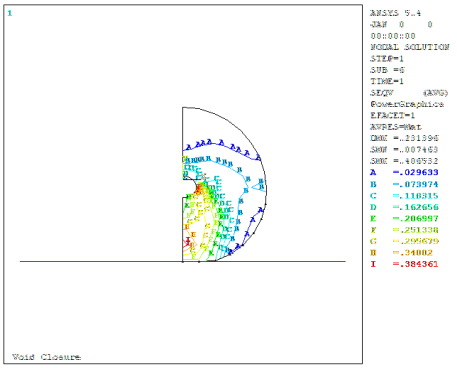

Fig. 37

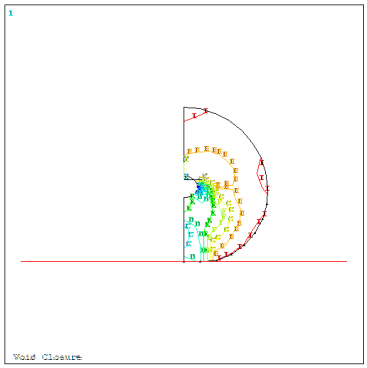

Fig. 34

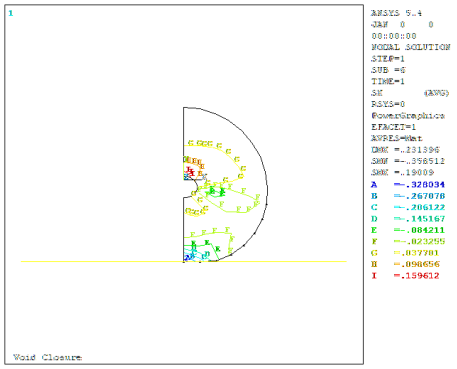

Fig. 38

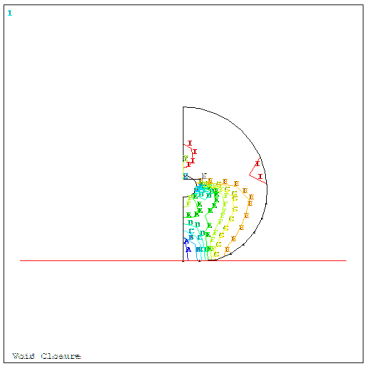

Fig. 39

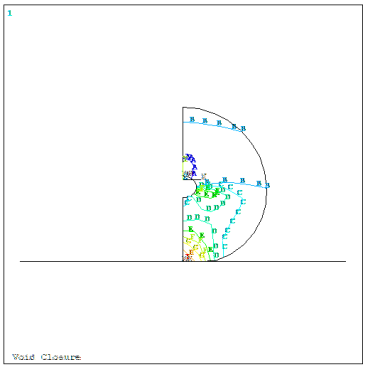

Fig. 40

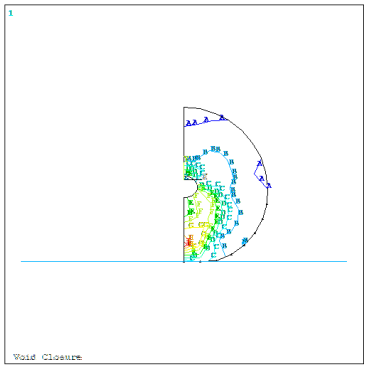

Fig. 41

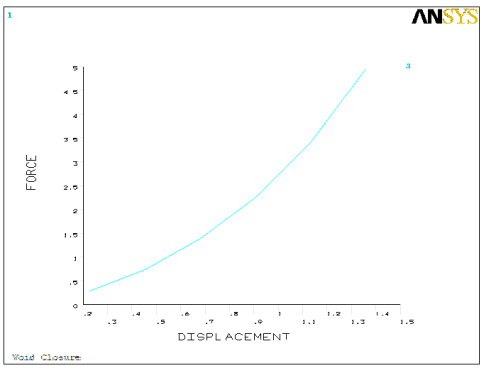

Fig. 42

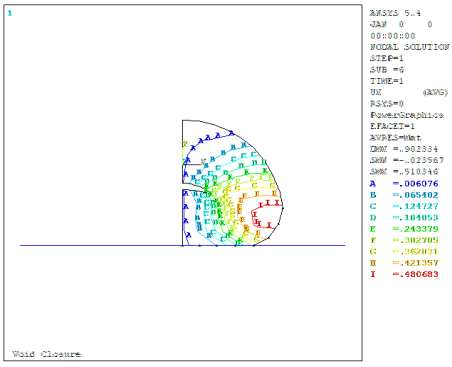

Fig. 43

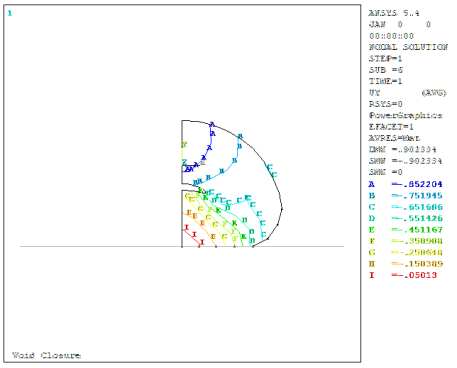

Fig. 44

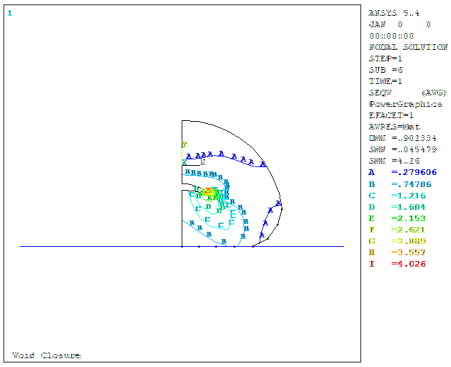

Fig. 45

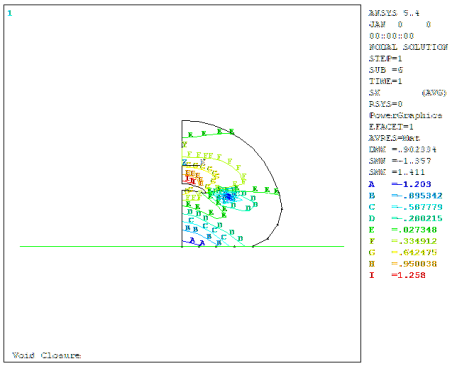

Fig. 46

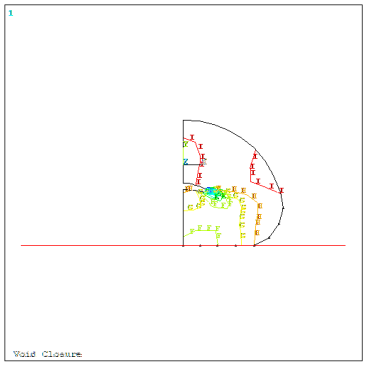

Fig. 47

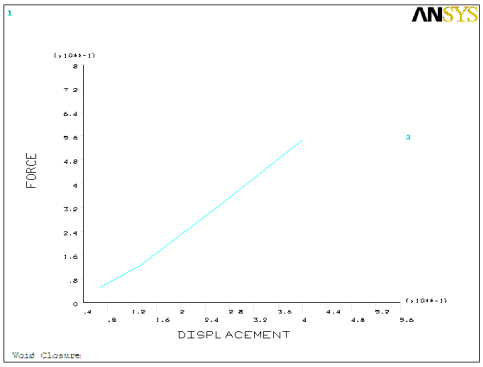

Fig. 51

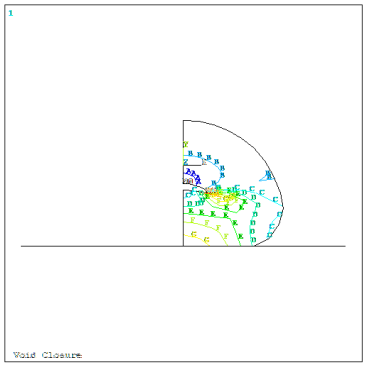

Fig. 48

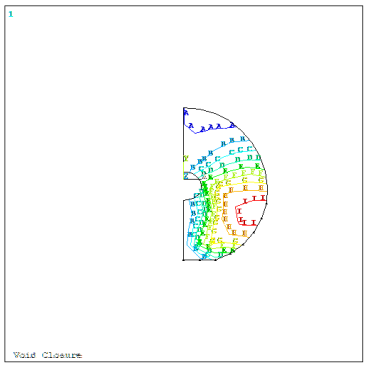

Fig. 52

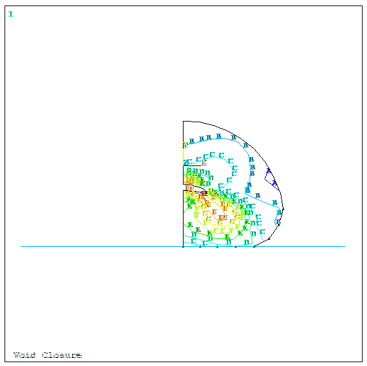

Fig. 49

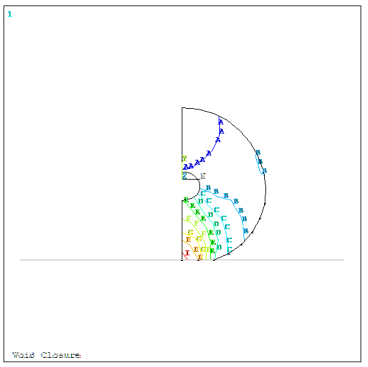

Fig. 53

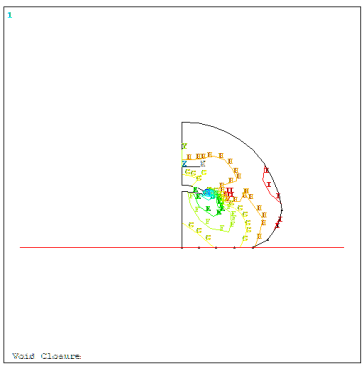

Fig. 50

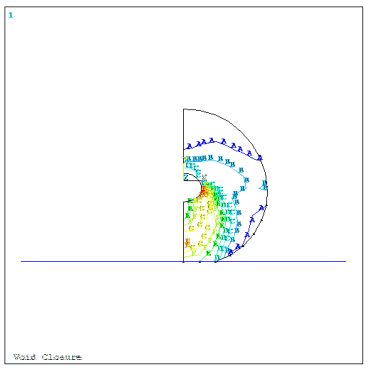

Fig. 54

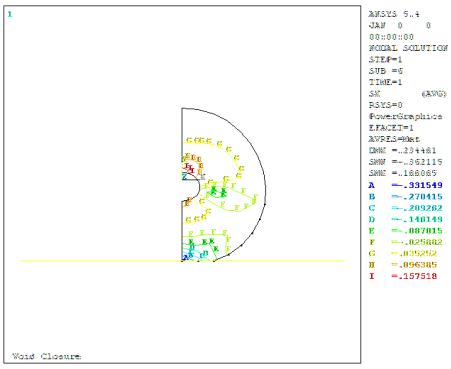

Fig. 55

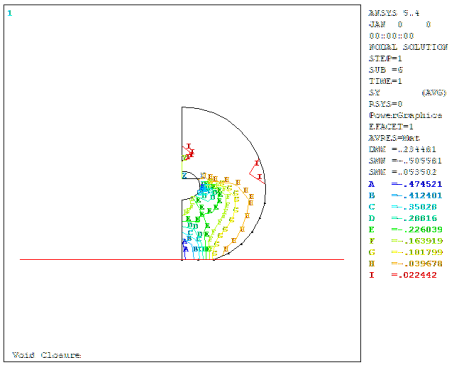

Fig. 56

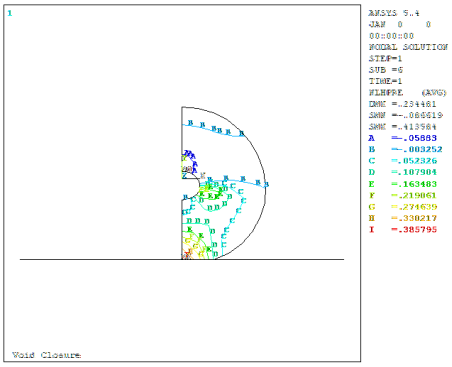

Fig. 57

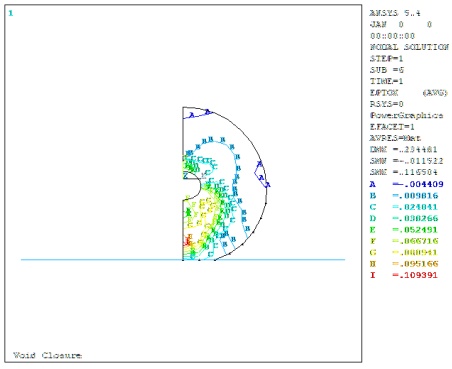

Fig. 58

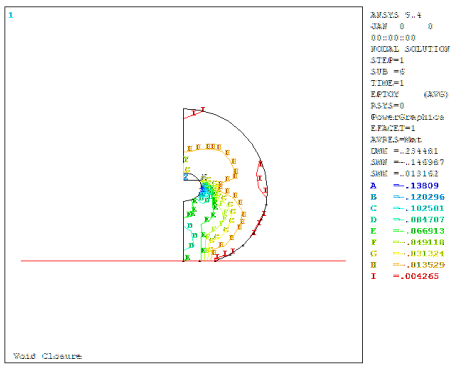

Fig. 59

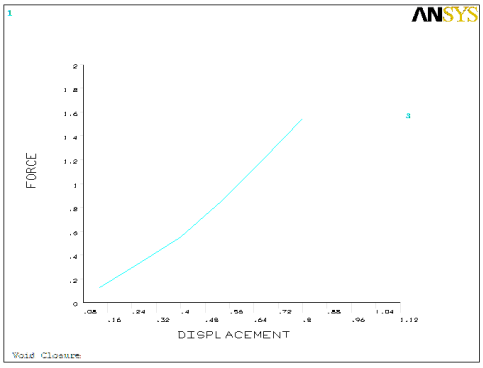

Fig. 60

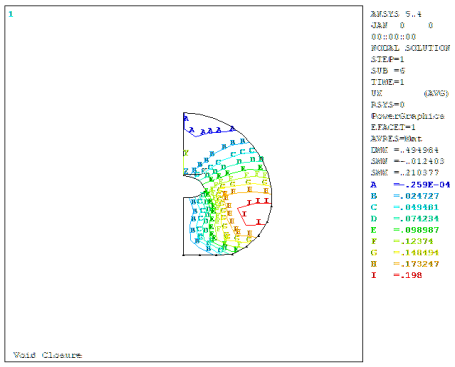

Fig. 61

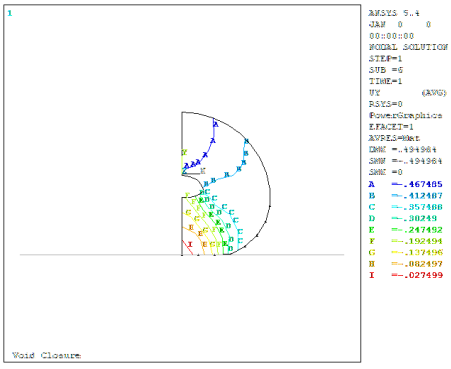

Fig. 62

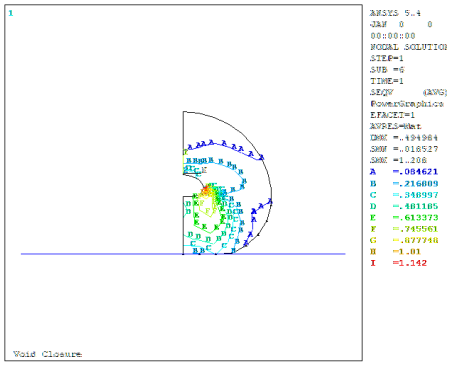

Fig. 63

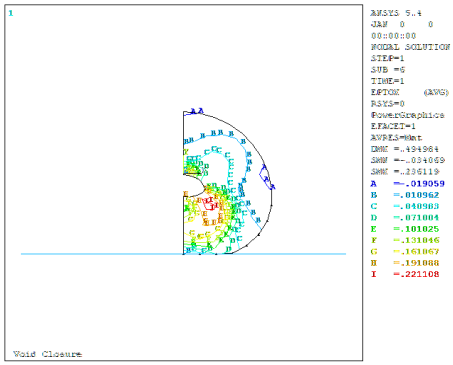

Fig. 67

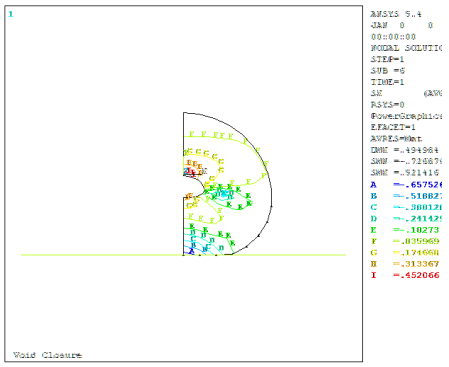

Fig. 64

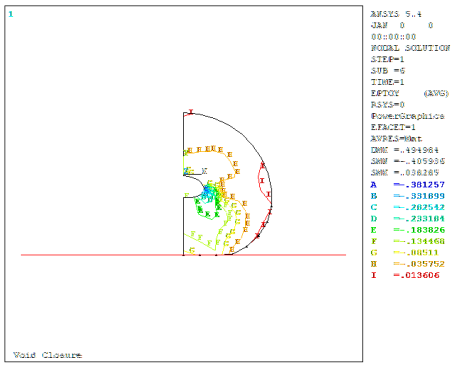

Fig. 68

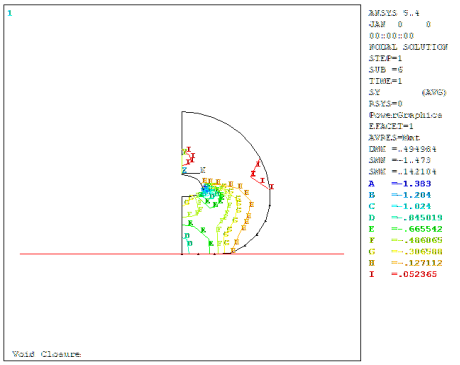

Fig. 65

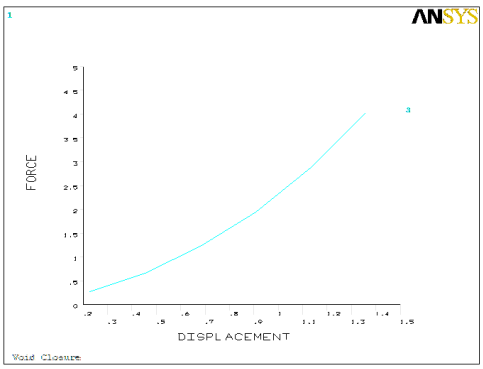

Fig. 69

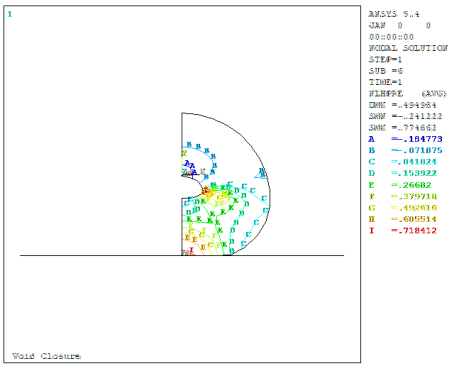

Fig. 66

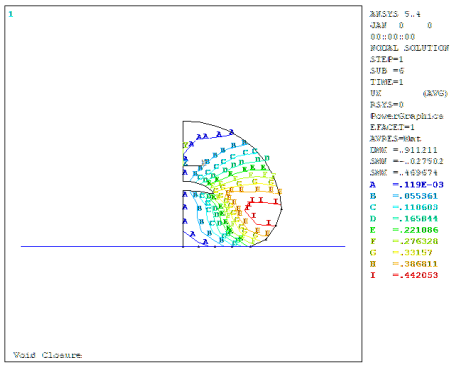

Fig. 70

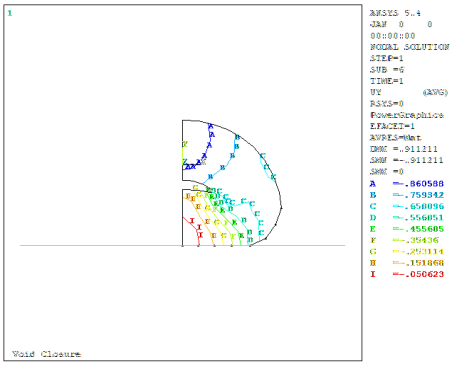

Fig. 71

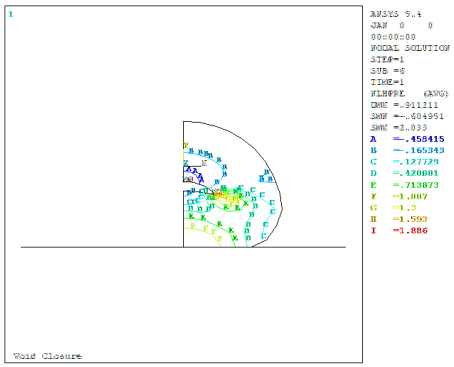

Fig. 75

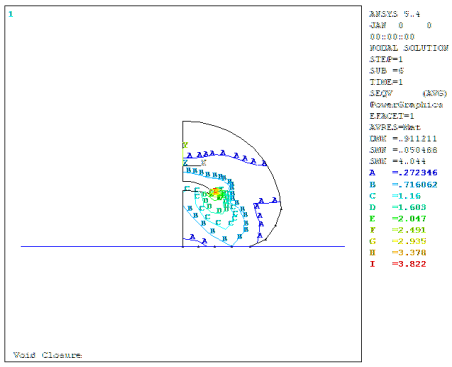

Fig. 72

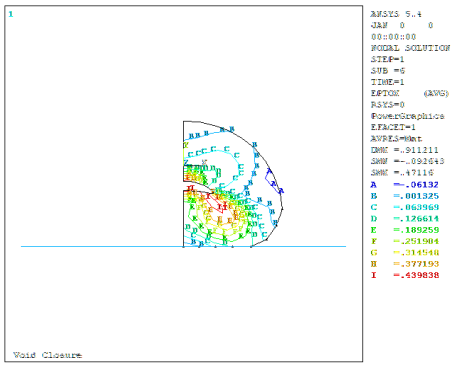

Fig. 76

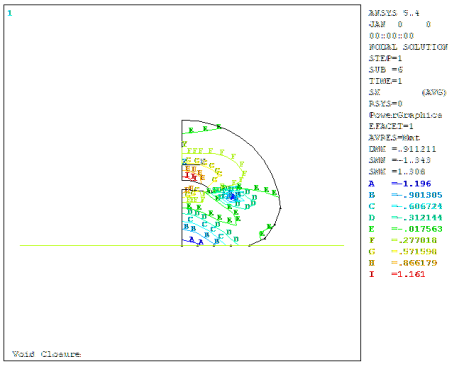

Fig. 73

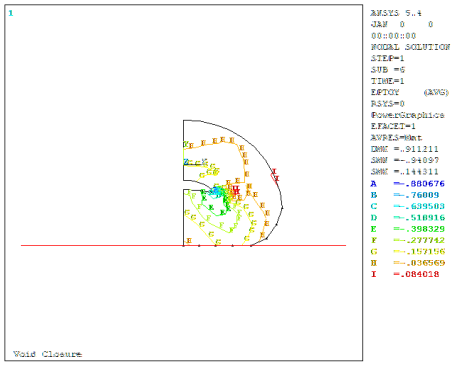

Fig. 77

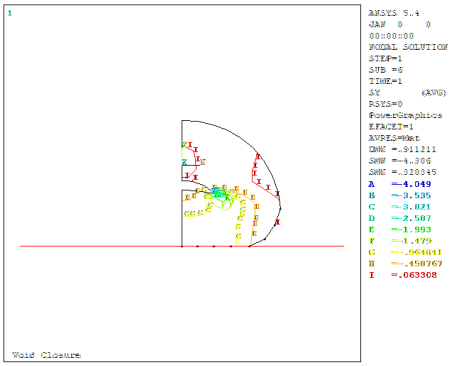

Fig. 74

5. Nomenclatures:

A0	Initial area (m^2)
Ai	Area at instance i (m^2)
B	Strain displacement relationship matrix
B	Transpose of strain – displacement relation matrix
D	Material properties matrix
Dmx	Max – displacement
ET	Element type
E	Young's modulus (N/m^2)
Fx/Fy	External applied forces (N)
K	Bulk modules (N/m^2)
Ke	Stiffness matrix for element e
N	Number of nodes
Px,Py	Pressure in direction x & y (N/m^2)
Pi	Pressure at instant i (N/m^2)
Smin,Smax	Minimum & maximum stress
T	Thickens of the specimen (m)
T	Time (sec)
E	Strain vector
S	Displacement vector (u1, v1, u2, v2, u3, v3, u4,v4) m
X	Functional
U	Total energy (joule)
Q	Unit matrix
σ_e	Equivalent stress (N/m^2)

6. References:

[1] Charles Barre "HIP increasing by used for upgrade of casting as process becomes economical "reprint from Incast. August, 1998, Kitty Hawk Product,1165,Monarch St. Garden.

[2] Dudra ,Steve and Taek, Yong " Analysis of void closure "Int. J. of Machine tools manufacture pp.711-780 (1982) .

[3] Sun Jie –Xian "Analysis of special forging processes for heavy ingot by Finite element method " Int. J. Mach .Tools Manufacture Vol. 28, No. 2 pp 173-179,1988.

[4] OH,S. I," Finite element analysis of metal forming processes with arbitrary shaped dies " Int. J. Mech. Sci. vol. 24, No. 8 pp. 479-491 (1982) .

[5] Mujkwan Kak Ajang "The effect of die shape on void closure in open die forging " Phd thesis, September ,2002.

[6] Cook,Robert, D. "Finite Element Modeling for stress analysis" 1995, John Willy and Son. Inc., New York.

تأثير شروط التشكيل مثل السرعة على غلق الفجوات بقوالب الطرق المفتوحة

علاء حسن علي
قسم هندسة المواد/ الجامعة التكنولوجية

الخلاصة

يقدم هذا البحث دراسة في تاثير السرعة على غلق الفجوات بمختلف أحجامها في المصبوبات، وقد تم استخدام طريقة العناصر المحددة في التحليل وتمت عملية التمثيل لمقطع اسطواني لمصبوبة تحتوي على تجاويف مركزية مختلفة الأحجام . تم التحليل على اساس ثنائي الأبعاد باستخدام قالب طرق مفتوح، وتم الحصول على النتائج لأغراض المقارنة وإيجاد أفضل انغلاق للفجوة باحجام مختلفة وسرع تشكيل مختلفة.